MODEL BASED DESIGN AND EXPERIMENTAL VALIDATION OF ELECTRO-MECHANIC ACTUATOR SYSTEMS FOR A NOSE LANDING GEAR

Dennis Doberstein, Frank Thielecke
Hamburg University of Technology - Institute of Aircraft Systems Engineering
dennis.doberstein@tuhh.de; frank.thielecke@tuhh.de

Keywords: *landing gear actuation, electro-mechanic actuator, kinematic, system design*

Abstract

In this paper the complete design and development process of an electro-mechanic actuation system (EMA) for extension and retraction of a nose landing gear is presented. Thereby novel kinematic concepts are introduced regarding a low actuation load to reduce size and weight of the actuator. For a favorable concept the model based design and dimensioning process of a suitable EMA are described. The functionality of the concept is demonstrated in a test rig.

1 Introduction

Today's commercial aircrafts landing gears are typically actuated by hydraulic cylinders which are supplied by the aircrafts central hydraulic system. These systems show quite high energy losses in operation due to velocity control by hydraulic orifices and servo valves. Furthermore, the actuation time depends on the external loads.

The concept of a *More Electric Aircraft* (MEA) offers perspectives in terms of performance, energy consumption and safety by using efficient electric actuators and an electric energy distribution combined with a sophisticated power management. Past projects, like POA (*Power Optimized Aircraft*) or MOET (*More Open Electric Technologies*), already put a great effort into the development of *Power by Wire* (PbW) actuators and led for example to the electro-hydrostatic actuator technology (EHA), which is already used in primary flight control in the A380, [2], [3], [8].

Relating to the concept of a MEA, for landing gears it is also considered to replace the hydraulic actuators by electro-mechanical components, as the landing gear extension and retraction function is one of the main energy consumers.

However, first studies carried out that it is not useful to substitute the hydraulic actuators directly by their electric counterparts. Reasons are the different characteristics and dynamic behavior of hydraulic and electric drives. In general, hydraulic cylinders are able to generate high forces, whereas the actuator is quite small in weight and size. Arranging electro-mechanic actuators (EMA) in the same position would result in a much higher system weight and require more space due to their lower power density. Hence, a redesign in kinematic and actuator configuration is appropriate for the change from hydraulic to electric power supply to make the EMA system competitive to the state of the art.

Furthermore, new system solutions have to be found to fulfill the specified system functions. For example a passive emergency extension mode (*freefall*) is required in case of a loss of energy supply. In this case, the conventional cylinder is hydraulically damped by a throttle valve between the cylinder chambers to limit extension speed and thus to prevent structural damage. This option is not available when using an EMA.

The paper follows the subsequent structure: Section 2 briefly describes an exemplary nose landing gear actuation system for the experimental investigations and names the design requirements considered in this process. Section 3 shows different variations for the integration of a rotary EMA into the conventional landing gear structure. One main goal of the development process is to design a novel

kinematic with a low actuation load to reduce actuator size and weight. Based on the results of this analysis, a concept with a rotary EMA is chosen for further analysis. Actuator components and other system elements like the locking springs are dimensioned in consideration of the system specification in section 4. Afterwards, an overall simulation model of the landing gear actuation system is created in MATLAB-SIMULINK, including a simplified multi-body model of the landing gear structure. The simulation model is used to design an electric damping mode by using the electric motor in generator mode combined with a break resistor. To proof functionality of the concept, the Institute of Aircraft Systems Engineering built a test rig of the developed nose landing gear system. The test rig and experimental results are described in section 5.

2 System Description and Modeling

The analysis is based on a common nose landing gear (NLG) structure as shown in fig. 1. Hydraulically actuated NLGs are in general implemented as a six-link coupler mechanism. As the main component, the *main strut* transfers the major part of the ground loads to the fuselage and furthermore includes the damper, nose wheel steering and the wheels subsystems. It is braced against the fuselage in extended position by the *drag brace*, which divides into the upper and lower drag brace. The passive downlock mechanism is realized by the *locking stay* which is overcentered against a mechanical end stop in extended position, supported by the locking springs. It reduces the degree of freedom of the system to zero in down position and engages automatically without assistance from the hydraulic system. An unlock actuator is implemented to open the downlock.

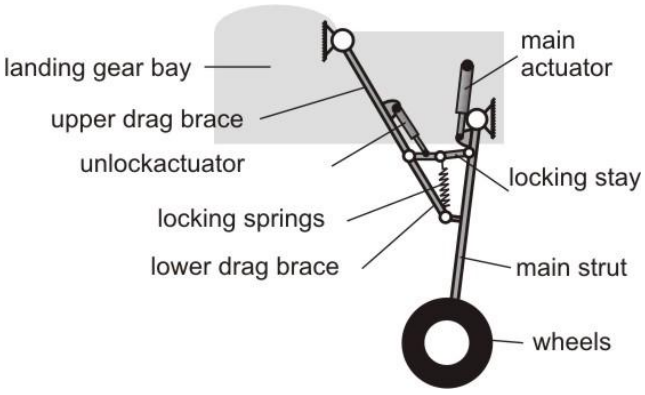

Fig. 1. General Aircraft NLG System

2.1 System Requirements

Different types of requirements have to be taken into account. These are listed in the following paragraphs.

2.1.1 Functional Requirements

The NLG actuation system considered in this design process shall fulfill the following system functions:

- extension and retraction under normal operating conditions
- emergency extension (*freefall*)
- uplock
- passive downlock without actuator assistance

The steering system is not considered here.

2.1.2 Performance Requirements

The *European Certification Specifications for Large Aeroplanes* (CS-25) of EASA do not specify any actuation time limits. Instead, in general these are defined individually relating to the specific aircraft concept. Typically, the actuation times vary between 10 s – 15 s, [5]. Based on this information, the system shall meet the following actuation time requirements:

- retraction (normal operation) < 10 s
- extension (normal operation) < 13 s
- retraction (limit operation) < 13 s
- extension (limit operation) < 15 s

The differentiation between normal operation and limit operation refers to different flight conditions which are described in the following section.

2.1.3 Actuation Loads and Load Conditions

The actuation loads comprise several load components.

The following operating loads are considered for this design process:

- weight
- g-loads, resulting from flight maneuvers
- aerodynamic loads
- spring loads
- joint friction

These operating loads are specified for different load cases which represent specific flight conditions. Varying parameters like the aircraft speed result in varying aerodynamic loads, for example. For this system design only limit loads are taken into account since these are relevant for actuator sizing. The relevant load cases are summarized as follows:

- total actuation torque under limit operating conditions
- total actuation torque under normal operating conditions
- minimum actuation torque combined with reduced power supply (one engine inoperative, minimum aircraft speed)

2.2 Multi-Body Modeling

As mentioned before one main goal of the kinematic redesign is to achieve a low actuation load. Landing gear kinematics are transmission gears with a varying transmission ratio along the retraction angle. These coupler mechanisms can be analyzed analytically or by application of specific numerical optimization tools for mechanical linkage systems. [6] describes methods and tools for the analytical kinematic optimization of a landing gear system with a rotary EMA.
However, these tools only consider the kinematic ratio between actuator output and main strut. Dynamic effects or variations of external loads cannot be taken into account. For this reason, the method of *multi-body simulation* (MBS) is used for the landing gear design at this point. This method allows to model and study the dynamic behavior of a system of rigid bodies and to consider the influence of external and internal force elements, like for example joint friction or springs. A simplified multi-body model of the reference system is shown in fig. 2.

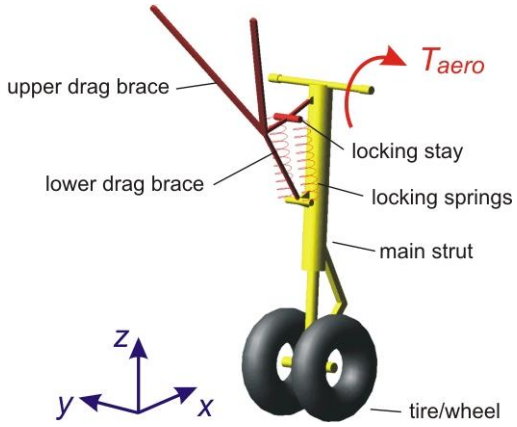

Fig. 2. Multi-Body Model Of NLG

It is created in the MBS-software MSC.ADAMS. It can be seen that the NLG is represented by simplified homogeneous solids. Nevertheless, their mass properties as well as their dynamic properties are defined with respect to the original elements. All actuation loads described in Sec. 2.1.3 are taken into account in this model. The actuators are not implemented at this point.

3 Integration Study for EMAs

Due to the desired rotational output movement, a rotary EMA appears to be an appropriate choice for this application. In this section, exemplary solutions for the integration of a rotary EMA into the basic kinematic are presented and evaluated. Linear actuator concepts are not taken into account. Any design has specific positive properties which are described in the following.

3.1 Novel Kinematic Design

Fig. 3 shows three different concepts to integrate a rotary actuator into the basic landing gear kinematic. The position of the rotary EMA is marked with ‘A’. In variation A, the actuator is located at the upper drag brace pin. Contrary to the original system, the drag brace is rotating in forward direction.
Variation B is based on the original system, the downlock mechanism and kinematic are maintained unchanged. The actuator is linked directly to the locking stay by two additional link elements. This approach does not require an

additional unlock actuator because the locking stay is raised by the actuator link itself.
Variation C is an advanced architecture of concept B. The locking stay is replaced by the actuator link elements which are directly connected to the drag brace apex joint. The downlock function is adopted by the actuator link as well.

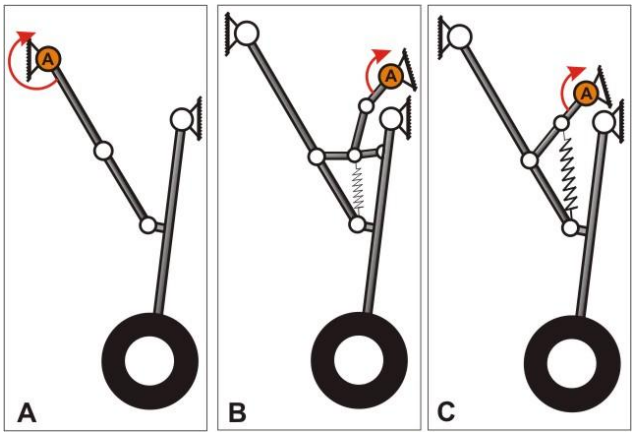

Fig. 3. Novel Kinematic Concepts

3.2 Torque Analysis and Design Evaluation

The determination of the maximum required actuator torque is done by MBSs of the concepts A-C, considering the limit operating load case. The optimal actuator positions and joint locations are estimated by using an empirical design optimization tool included in the MBS software, based on the method of *design of experiments*. This optimization tool runs several simulations in a batch-run while the values of defined design parameters are varied systematically. It returns the design parameter set which fulfills best the desired design criterion. Fig. 4 summarizes the actuator torque curves of the optimized kinematic concepts. The torque values are normalized to the maximum torque (T_{max}) of the reference system (Ref). The reference curve refers to a rotary actuator in the pivot of the main strut. It can be seen that all variations show an improvement on the reference concept, regarding actuator torque. The maximum torque of concept A is lowest due to the big rotation angle the actuator has to travel to get in full up position. This leads to a good transmission ratio between EMA and main strut rotation. Concept C shows a favorable flat

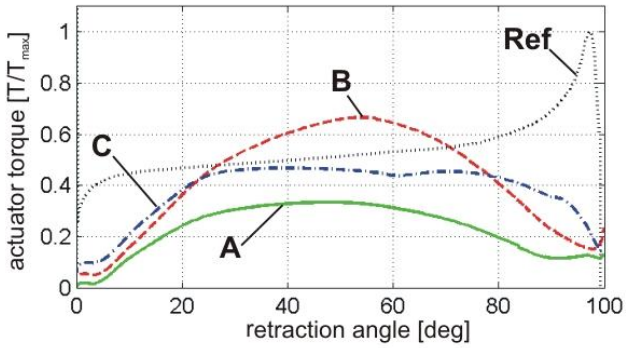

Fig. 4. Required Actuator Torques Of Optimized Concepts A-C

torque curve which means that the actuator would be well dimensioned for the whole operating range and not be oversized.
Nevertheless, more factors than the maximum actuator torque have to be taken into account for selection of a preferable concept. Concept A, for example, offers no options for the integration of locking springs to realize a passive downlock. Furthermore it requires big installation space due to the large rotation angle of the upper drag brace in forward aircraft direction. Concept B leads to a big increase of complexity.
The relevant evaluation parameters and results of the evaluation process are listed in tab. 1. It verifies concept C as best regarding the criteria described above. Because of this, concept C is chosen for further system design.

Tab. 1. Evaluation Matrix For Concepts A-C

Criterion	Weight	A	B	C
Passive downlock	5	1	3	3
Required torque/ load curve	4	3	1	2
Complexity	3	2	1	3
Installation space	2	1	2	2
Total		**25**	**26**	**36**
Explanation: 1: bad 2: neutral 3: good				

4 System Component Design and EMA Modeling

4.1 Actuator Sizing

The dimensions of a drive are assigned by required torque and speed. The maximum

required actuator torque is already determined by the analysis in sec. 3.2 with the limit operating load case. The maximum required actuator torque is the relevant parameter which defines actuator size and hence the weight.

The maximum retraction angle of the landing gear is assumed to be 100 deg. According to the determined kinematic, the maximum actuator output rotation angle amounts to 190 deg. With reference to the minimum retraction time in sec. 2.1.2 it is assumed that a complete run from 0 deg to 190 deg shall take no longer than 8 s to take into account acceleration and deceleration effects. This results in a required EMA output speed of at least 24 deg/s.

Electric drives usually attain their highest degree of efficiency at high motor speeds. Due to the low required output speed in this application, the use of a high reduction gear is essential. As an electric drive, brushless DC servo motors appear reasonable in this case since in general, they have a high efficiency and require low maintenance due to the lack of brushes. Furthermore, they can be well controlled and have a high dynamic. According to usual manufacturer information, the optimal operating speed of brushless DC motors is at around 4000…6000 rpm (f.ex. [9]). With the required output speed determined above, the aspired gear ratio i_{EMA} results to around 1000…1500.

Among others, an example for high reduction gears is the principle of HARMONIC DRIVE gearboxes. HARMONIC DRIVE gearboxes offer gear ratios up to more than 150 in a single stage, combined with high precision and low weight, [9]. For this reason the HARMONC DRIVE gears appear suitable for this application.

Nevertheless, in any case a second reduction stage is necessary to achieve the aspired total ratio i_{EMA} named above. In this case, this is realized by a conventional planetary gear arranged between motor and HARMONIC DRIVE. With the total ratio of a selected gear combination and the sizing parameters given above, a suitable electric drive can be chosen.

4.2 Overall System Modeling

As a model based approach is objective for further system design and analysis, a complete simulation model of the landing gear, comprising EMA and kinematic, is necessary. However, as the possibility to implement and represent both the electric and control system of the EMA in the applied MBS software in required detail is not sufficient, a model of the EMA is built in MATLAB-SIMULINK (according to [6]).

In this application, the electric drive is operated in velocity control mode with a rotational speed command. The control system of the electric drive is a cascade structure, as typical for brushless DC motors. It consists of the current controller in the inner cascade and the velocity controller as the outer cascade. The mathematical description of the motor is performed in a reduced two-phase *d-q* coordinate system according to [1] and [10]. The two gear elements (planetary gear and HARMONIC DRIVE gear) are represented each as simplified spring-damper elements with specific ratios, inertias and efficiencies, in accordance with [4] (fig. 5).

After this, a model representing the EMA in sufficient detail in MATLAB-SIMULINK and a multi-body model of the landing gear kinematic in MSC.ADAMS are available. The interaction between these two models could be attained by a co-simulation between MATLAB-SIMULINK and ADAMS. However, in this case the aim is to run the simulation in a common software environment for simplified handling

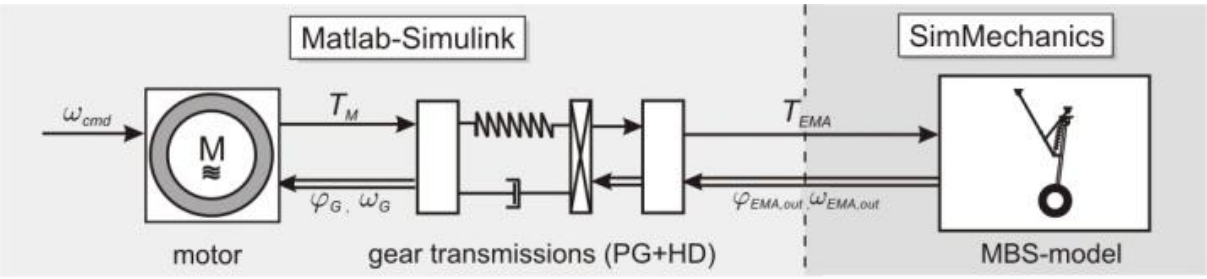

Fig. 5. Simplified Structure Of Overall NLG System Model

and in order to reduce computing time. The design tools provided by ADAMS are not needed anymore as the kinematic is fixed at this point. For this reason, the multi-body model of the NLG in ADAMS is transferred to a simplified kinematic model in the MATLAB-Toolbox SIMMECHANICS, in analogy to [6]. SIMMECHANICS only provides very limited features for kinematic design and optimization. However, the dynamic behavior and physical characteristics are represented sufficiently.
Fig. 5 shows the simplified structure of the overall system model. As the kinematic model in SIMMECHANICS requires the torque T as input variable, in contrast to [4] T is the forward input variable within the model structure. The angular velocity ω and angular position φ are feedback parameters.

4.3 Actuator Friction Estimation

The internal friction losses of the actuator elements, especially the gearboxes, have a major influence on the dynamic system behavior. Particularly the required back drive torque of the actuator must be taken into account due to the high transmission ratio, regarding a passive emergency extension. For this reason, the objective is to describe the EMA friction as accurately as possible. Therefore, a friction estimation experiment is done.
For friction determination, the actuator unit is measured stand alone on a test rig. The simplified experiment set-up is shown in fig. 6. The EMA is fixed on a frame and the output shaft of the EMA is equipped with a pinion. A load can be generated by a hydraulic cylinder which acts on the pinion via a rack. The load unit is force controlled using a load cell between the piston rod and rack. For determination, it is assumed that the whole actuator friction occurs

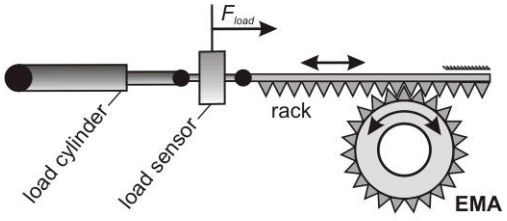

Fig. 6. Setup Friction Estimation Experiment

within the following three actuator elements: motor, planetary gear and HARMONIC DRIVE. However, the proportion on the elements is not specified.
The electric torque of the motor is named with $T_{mot,el}$, the load torque on the EMA output is T_{load}. With these parameters and the total gear ratio i_{EMA}, the actuator friction can be determined as:

$$i_{EMA} \cdot T_{mot,el} - T_{EMA,fric} = T_{load.}$$

In this calculation, the torques are related to the actuator output. Due to the lack of a load sensor in the motor, the electric torque $T_{mot,el}$ cannot be measured directly. Instead, it is estimated by the motor current I_{mot}. Usually, this method leads to a high inaccuracy due to the typically high tolerance of the torque constant k_t [Nm/A] which is usually provided by the manufacturer. However, for this determination a specific and more precise transfer function is available from a previous measurement series. It represents the relation between motor torque and current as a function of speed and temperature for the motor used in this application. This estimation is assumed as being sufficient.
The measurement is performed at different operating conditions, varying in motor speed, actuator load and operating temperature. The goal is to create a friction map for the EMA based on a frictional function which calculates the EMA friction depending on a specific combination of motor speed, actuator load and operating temperature. The temperature range covers the whole aircraft operational temperature envelope of -40 °C to +52 °C.
As an example, fig. 7 shows the results for an operating temperature of 20 °C. The measurement points are shown together with the approximated function at 4 loadcases (T_{load} = 0 Nm; 3 loadcases T_{load} > 0 Nm). The friction function is determined regarding the best fit to the measurement data over the entire operating range. Different friction effects are not represented particularly in the friction function.
The approximated function confirms the different friction characteristics of driving operating mode (n_{Mot} > 0 rpm) and backdrive operating mode (n_{Mot} < 0 rpm). According to the measurement data, the friction losses in braking

operating mode are exceptional small. Usually the back drive efficiency is expected to be higher in driving mode. An explanation for this effect thus far is not available. Nevertheless, the experimental validation confirms the friction model (sec. 5).

The friction torque characteristic in driving operating mode (n_{Mot} > 0 rpm) corresponds roughly to a classic "STRIBECK-curve" which takes into account viscous and coulomb friction. Static friction is not represented in this approximation due to the small number of measurement data at low speeds. The friction torque in back drive mode (n_{Mot} < 0 rpm) differs strongly from this characteristic. Regarding the few measurement points, the beginning of a very heavily stretched "STRIBECK-curve" can be divined. Even static friction can be recognized at about -500 rpm motor speed. In conclusion, at positive motor speed the fast rotating actuator elements, like motor and planetary gear input, are dominant for the friction losses. In back drive operating mode the friction characteristic depends on the slow moving elements, in the particular case the HARMONIC DRIVE output.

The friction function is implemented as an additional SIMULINK-block into the EMA model. At any simulation time step, it uses the current parameter values to calculate the current EMA friction torque.

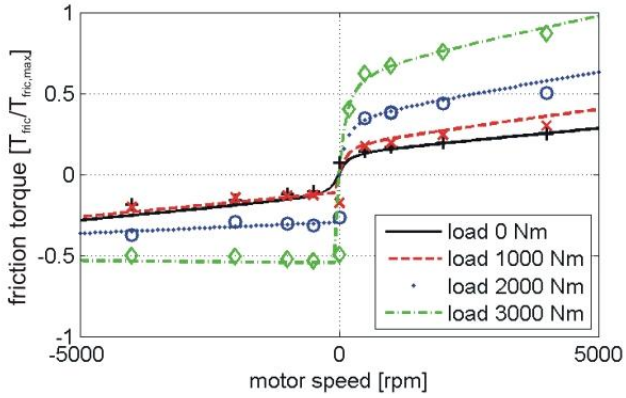

Fig. 7. Results Of Friction Estimation Experiment

4.3 System Component Design Regarding Emergency Extension

As mentioned in sec. 2.1.1, an emergency extension mode (*freefall*) is required in the event of loss of energy supply for the actuation system. In this operating mode, the actuator is assumed to be passive and the landing gear extends by gravity and external loads. However, the hydraulic damping option of the conventional system is not available when using an EMA. Certainly, an undamped extension event would result in serious structure damage. [7] illustrates the results of an undamped emergency extension system simulation. It shows that motor speeds up to 15000 rpm can occur which significantly exceeds the mechanical speed limit of common servo motors. At this point, the possibility to generate an appropriate braking torque by the passive actuator is examined.

4.3.1 Locking Springs Sizing Requirement

The idea of generating a braking torque in freefall mode by the passive actuator means that the EMA has to remain connected to the landing gear structure during emergency extension. Hence, the requirement for a reliable freefall is that under any operating conditions the passive actuator must be able to be backdriven by external loads. For this case, the minimum actuation loads (sec. 2.1.3) have to be taken into account.

The required backdrive torque of the EMA mainly results from its internal friction losses and was already determined in sec. 4.2. As common for NLGs, its weight and aerodynamic loads support the extension movement and thus generate a backdrive torque for the actuator. However, kinematically the transmission ratio from the actuator to the main strut reduces to zero at full extended position. This is illustrated by the load curve in fig. 4 which is zero at retraction angle zero. This means that near the extended position, the external loads stated above have no force on the actuator. Instead, only the locking springs (compare fig. 3) ensure an extension movement. As their effective lever arm on the actuator is smallest in extended position, the simplified sizing requirement for the springs is that their resulting torque on the actuator in extended position has to be greater than the actuators backdrive torque.

Fig. 8 proofs this freefall condition for the minimum actuation load case (sec. 2.1.3). The

locking springs are suitable sized for the system considered in this case.

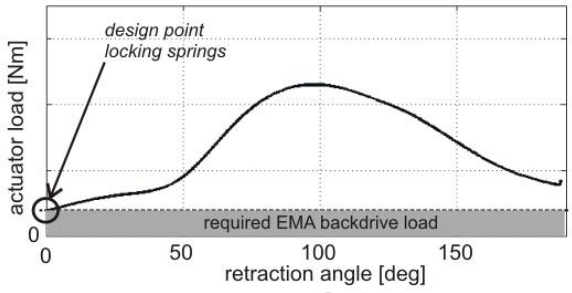

Fig. 8. Backdrive Load On EMA in Freefall Mode

4.3.2 Passive Emergency Extension Design

Usually, brushless DC servo motors in braking operation mode feed back the energy absorbed from the system into the DC circuit. However, this requires a continuous energy supply of the inverter. As the emergency extension shall be performed in case of a loss of energy, in this application a braking operation mode with a passive electric network is considered. This mode is also used as emergency stop of industrial machines in case of loss of energy supply, [12].

In this mode, a control of the braking torque is not possible. It is determined only by the properties of the motor windings. A description of the braking torque of a passive servo motor is given in [11] and applied in [7].

The braking torque of the motor depends on its rotational speed, with a maximum torque at the stall speed n_{stall}. A system simulation of the motor used in this application shows its characteristic speed-torque-curve (fig. 9) which confirms the description in [11]. The dynamic behavior can be influenced in the desired way by inserting a suitable brake resistor into the three motor phases.

5 Experimental Validation and Proof

For verifying and proof of functionality of the developed system, a test rig was built at the Institute of Aircraft Systems Engineering at the Hamburg University of Technology. In the following sections the test rig is described and test results of a retraction procedure are shown.

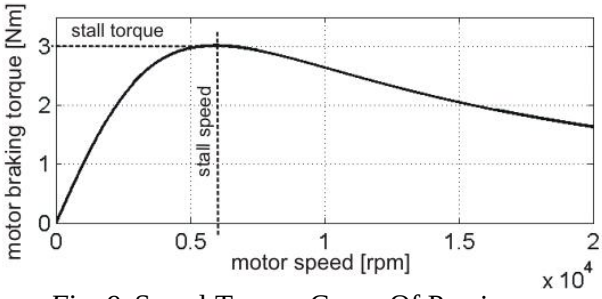

Fig. 9. Speed-Torque-Curve Of Passive Brushless DC Drive

5.1 Test Rig Description

The test rig is shown in fig. 10. It represents the complete NLG retraction and extension system referring to concept C in fig. 3 with simulation of its external operating conditions. The landing gear elements consist of dummy components which represent the mass of the original elements. Due to the low development level, so far the actuator is realized by commercial industrial components. The landing gear is mounted in a frame which ensures sufficient space for the landing gear movement. In addition, a load cylinder is attached at the back of the main strut (not visible in fig. 10) to simulate aerodynamic loads.

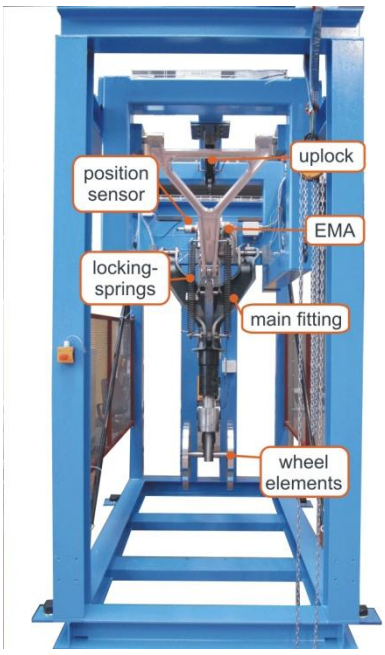

Fig. 10. NLG Test Rig For Electro-Mechanical Retraction And Extension

5.2 Test Results

To validate the simulation models used for system design on the one hand and to proof functionality of the actuation system on the other hand, in the following the results of the overall system simulation are compared to the test rig measurement.

5.2.1 Retraction

As regular operating mode, a normal retraction procedure at medium operating load (according to standard flight conditions) is considered. Fig. 11 compares the results of model simulation and test rig measurement.
The procedure is started at t_{start} = 1 s and reaches the end stop position at t_{stop} = 11 s (the delay in the test rig speed measurement results from an erroneous delay of the zero-speed detection). The total actuation time of 10 s satisfies the system requirements for normal operation in section 2.1. The electric motor is operated in velocity control mode with a constant speed command across a large range of the retraction angle to obtain a constant actuation time. Near the end position, the actuator speed is reduced for a soft end stop and hence to stay within the limit of the maximum acceptable end stop velocity. The speed command trajectory is defined in dependence of the actuator output angle which is determined by the motor encoder signal.
The recorded motor speed in fig. 11 proofs the good consistency of the dynamic behavior between test rig and model. However, it can be seen that the servo speed controller used in the test rig has a limited dynamic which explains the speed discrepancy at high motor torques. Nevertheless, this is no drawback for the system design. The controller in the test rig provides integral characteristic to stay within the actuation time limit. The motor torque shows a good correlation between test rig and model, as well. The differences result from the reduced controller dynamic mentioned before. Furthermore, the motor torque in the test rig involves a greater level of uncertainty because, due to a lack of installation space, it is not measured by a torque sensor but determined indirectly from the motor current signal.

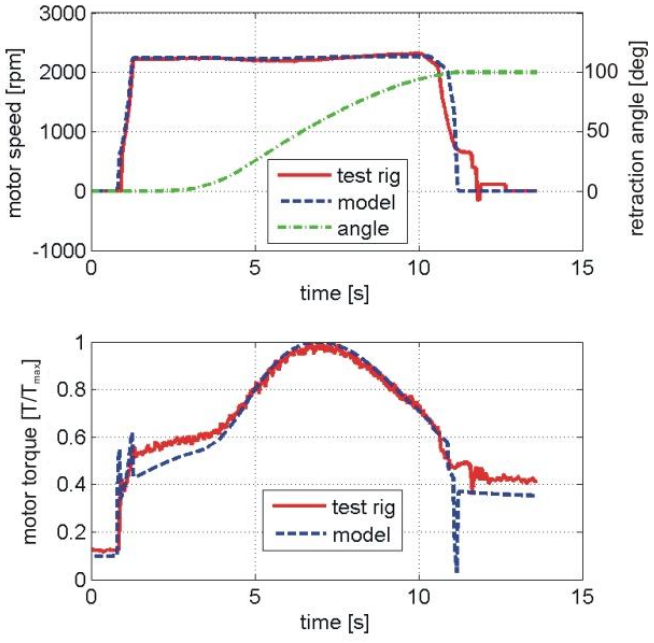

Fig. 11. Regular Retraction Procedure (Comparison Test Rig And Model)

5.2.2 Emergency Extension

Fig. 12 compares the motor speed measured in the test rig and the determined motor speed in the simulation model of a freefall test with low external loads. The extension time of 20 s resp. 25 s is quite satisfactory since no limit extension time is defined for this emergency procedure. It confirms the appropriate modeling of the passive actuator mode described in sec. 4.3.2. Furthermore it shows that a well sized brake resistor leads to a sufficient dynamic extension behavior.

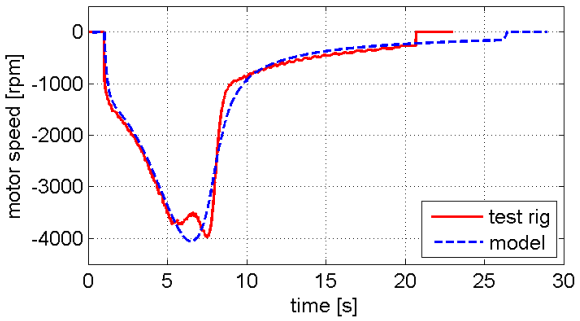

Fig. 12. Freefall Simulation And Test Rig Measurement

6 Conclusion

The design process described in this paper proves the general feasibility of landing gear actuation by size- and weight-optimized electro-mechanical actuators performing the required system functions. The kinematic design process is based on a multi-body simulation study of different landing gear structures using MSC.ADAMS. The result is a novel actuation kinematic with a rotary actuator which better suits the characteristics of EMAs regarding actuation torque and speed than a conventional architecture. An overall system model is implemented in MATLAB-SIMULINK, comprising the EMA model and a simplified kinematic model in MATLAB-SIMMECHANICS, for further system studies.

The actuator sizing ensures the compliance with the system performance requirements in normal operating mode. For the emergency extension mode, additional system components (like f. ex. locking springs) are designed to ensure an extension of the landing gear with backdriving of the EMA. An appropriate braking torque can be generated by the inactive servo motor to reduce extension speed and thus to prevent structural damage.

The system presented in this paper fulfills the general system functions. However, for application in a commercial aircraft, some major issues, especially regarding aviation-specific requirements, still remain unsolved. For example, qualification for low temperature operation as well as compliance with reliability of the actuator are still questions that have to be analyzed.

References

[1] Bonfert K. *Betriebsverhalten der Synchronmaschine*. Publisher: Springer Vergla, Berlin, Germany, 1962.

[2] vdBossche D. The A380 flight control electro-hydrostatic actuators, achievements and lessons learnt. *Proceedings of the International Congress of the aeronautical sciences (ICAS).* ICAS 2006-7.4.1, Hamburg, Germany, September 3-8, 2006

[3] Chevalier P.-Y, Grac S, and Liegeois, P.-Y. (2010), More electrical landing gear actuation systems. *Proceedings of the International Conference on Recent Advances in Aerospace Actuation Systems and Components (R3ASC).* pp 9-16, Toulouse, France, May 5-7, 2010

[4] Cochoy O, Carl U and Thielecke F. Integration and control of electromechanical and electrohydraulic actuators in a hybrid primary flight control architecture. *Proceedings of the International Conference on Recent Advances in Aerospace Actuation Systems and Components (R3ASC).* pp 1-8, Toulouse, France, June 13-15, 2007

[5] Currey N. *Aircraft Landing Gear Design: Principles and Practices*, AIAA Education Series, Marietta, GA, 1988

[6] Doberstein D, Thielecke F, and Renner O. *Methodik zum Entwurf einer Betätigungskinematik mit rotatorischem Antrieb für ein Fahrwerksystem*. Deutscher Luft- und Raumfahrtkongress. DLRK2009-1261. Aachen, Germany, September 08-10, 2009

[7] Doberstein, D. and Thielecke F. *Methodik zur Systemauslegung für ein elektrisch betätigtes Bugfahrwerk*. Deutscher Luft- und Raumfahrtkongress. DLRK2010-1272. Hamburg, Germany, August 31- September 02, 2010

[8] Faleiro L. *Beyond the More Electric Aircraft*, Aerospace America (AIAA), Vol 43 pp 35-41, Reston VA, September 2005

[9] Harmonic Drive. *Precision in Motion - General Catalogue*. Product Catalog. Harmonic Drive AG, Limburg, Germany, 2010

[10] Neuheuser T. Holert B and Carl U. *Elektrische Antriebssysteme für ein einzelnes Landeklappensegment*, Deutscher Luft- und Raumfahrtkongress, DLRK2002-192, Stuttgart, Germany, September 23-26, 2002

[11] Müller G. *Grundlagen elektrischer Maschinen*, Publisher: VCH Verlagsgesellschaft, Weinheim, Germany, 1994

[12] Vogel, J. *Elektrische Antriebstechnik*, Publisher: Hüthig Buch Verlag, Heidelberg, Germany, 1991

Copyright Statement